Development and mechanical characterization of novel ceramic foams fabricated by gel-casting

Citation: Tulliani, J.-M., M. Lombardi, P. Palmero, M. Fornabaio, and L.J. Gibson. "Development and Mechanical Characterization of Novel Ceramic Foams Fabricated by Gel-Casting." Journal of the European Ceramic Society 33, no. 9 (August 2013): 1567–1576.

As Published: http://dx.doi.org/10.1016/j.jeurceramsoc.2013.01.038

Publisher: Elsevier

Persistent URL: http://hdl.handle.net/1721.1/101907

Version: Author's final manuscript: final author's manuscript post peer review, without publisher's formatting or copy editing

Development and mechanical characterization of novel ceramic foams fabricated by gelcasting

J.M. Tulliani[1*], M. Lombardi[1], P. Palmero[1], M. Fornabaio[1], L.J. Gibson[2]

[1] Politecnico di Torino, Department of Applied Science and Technology, Corso Duca degli Abruzzi 24, 10129 Torino – Italy

[2] Department of Materials Science and Engineering, MIT, 77 Massachusetts Avenue, Cambridge MA 02139 –USA

Abstract

Porous ceramic materials are of considerable interest for a variety of chemical and industrial applications in extremely harsh conditions, particularly at very high temperatures for long times. A modified gelcasting process employing agar as a natural gelling agent and polyethylene spheres as pore formers was exploited to produce porous ceramic bodies. Alumina and alumina-ZrO_2 (AZ) powders were used to prepare samples having a porosity of about 65-70-75 vol%. The composite powder was produced by a surface modification route, i.e. by coating a well dispersed alpha-alumina powder with a zirconium chloride aqueous solution. Upon thermal treatment, ultra-fine tetragonal zirconia grains formed on the surface of the alumina particles. SEM observations and image analysis were used to characterize the microstructure of porous samples and uniaxial compressive tests were used to measure their mechanical behavior.

* **Corresponding author**: Jean-Marc Tulliani, Politecnico di Torino, Corso Duca degli Abruzzi, 24, 10129 Torino - Italy.
Tel: +39(0)11 564 47 00. Fax: +39(0)11 564 46 64. E-mail: jeanmarc.tulliani@polito.it

Key words: gel casting, alumina, composites, porous samples, compressive strength

Introduction

Porous and cellular ceramics find application in many industrial and biological processes, such as high-temperature thermal insulation, support for catalytic reactions, filtration of particulates from diesel engine exhaust gases and from hot corrosive gases, and bio-compatible scaffolds for bone substitution. In order to reach the desired properties, the development of a specific structure with controlled volume fraction, size, type and geometry of pores is required.

Complex ceramic shapes can be generally prepared through several methods. Green and fired parts can be machined to the desired shape; however, this is rather time consuming and very expensive especially for fired parts. Moreover, machining is not always applicable to complex shapes such as, for example, turbine rotors. Alternatively, complex shapes can be made by injection molding a ceramic powder in a vehicle of a polymeric or wax-like binder (such as paraffin, for example). This method, too, has disadvantages: the binder removal times are rather long and the process often induces cracks or warpage in the molded parts [1,2]. Slip casting techniques can be also used for the production of porous ceramics, but density variations can take place. In addition, these techniques give low-strength green bodies that cannot be easily machined prior to sintering.

To overcome the drawbacks of these preparation methods, and to satisfy the criteria of homogeneity, reproducibility, reliability and processability required for complex shape commercial ceramics, processing by gelcasting has been developed [3]. Gelcasting is a near-net-shape forming method that combines slip processing with polymer chemistry. It was initially set up using organic media [1] and then later, water [2]. In this process, a small amount of organic gel-formers are dissolved in water to obtain the so-called premix solution. Next, the ceramic powder is dispersed in the premix solution and then cast in a nonporous mold. As in other slip processes, efficient de-airing of the slip and careful mold filling are required to avoid the introduction of defects that may limit the strength and other physical properties [4]. By the action of temperature or/and chemical cross-linking reactions, the gel-formers create a strong polymer hydrogel, which permanently immobilizes the ceramic particles in the desired shape of the mold cavity. After demolding, the part is dried, then the polymer is burned out and the sample is sintered. Gelcast green bodies have a high strength, allowing them to be easily machined before sintering [5]. Moreover, the complexity of the shapes obtainable by gelcasting is limited only by the ability to design and fabricate the molds [4].

The original study on gelcasting involved polymerization of acrylamide monomers as gel-formers. Monofunctional acrylamide, CH_2=CHCONH$_2$ (AM) and difunctional N,N'-methylenebisacrylamide, (CH$_2$=CHCONH)$_2$CH$_2$ (MBAM) have been used as the reactive organic

monomers; however, industry has been reluctant to use acrylamide, as it is a known neurotoxin. Hydroxyethyl methacrylate (HEMA) [6], glycerol monoacrylate [7], acrylic acid [8], N,N-dimethyl acrylamide (DMAA) [9], epoxy resin [10], urea formaldehyde [11] and dimethylformamide [12], as well as alternative natural gelling agents, such as, for example, agar [13], agarose [13], carrageenan gums [13], egg white [14], chitosan [15], gelatin [16,17], sodium alginate [18], polyvinyl alcohol [19], glutin-urea [20] and glucose [21] have been extensively tested in these last years.
Environmently friendly natural gel-formers also have the advantage that their gelation takes place with changes in temperature (on heating with methylcellulose derivatives or on cooling with agaroids and gelatine) without the use of catalysts and initiators, as in the case of synthetic monomers.
Gelcasting was initially set-up for preparing dense components. More recently, the process was modified to fabricate porous ceramics, by combining it with foaming techniques [19], or sponge methods [22], or even exploiting particle stabilization with short chain surfactants [23], as well as adding a fugitive phase such as, for example, carbon powders [24], commercial polyethylene [25] or polystyrene [26] spheres. The pore forming agent is generally selected on the basis of its shape and size distribution and it is added into the slurry with a controlled volume fraction with respect to the ceramic content. In this way, it is then possible to strictly control the pore shape, size and volume fraction of the final ceramic components [25].
The current paper deals with the exploitation of a modified gelcasting process [25,27], using an agar as a natural gelling agent and polyethylene spheres as pore formers. Porous ceramic bodies made of pure alumina (A) and alumina-10 vol% ZrO_2 (AZ) were prepared, by employing a bi-phasic AZ powder obtained through a surface modification method [28-32]. Alumina-zirconia composite ceramics are widely used for various structural applications, due to their increased mechanical properties produced by the dispersion of fine ZrO_2 grains inside the alumina matrix. In fact, the dispersion of 5–20 vol% tetragonal zirconia particles in the alumina matrix can significantly improve the fracture toughness of the neat matrix due to the tetragonal/monoclinic transformation of the zirconia phase under loading [33-35]. Most of the current applications of alumina-zirconia composites are based on dense, fully sintered materials, without porosity. It is challenging, however, to use this composition also for the preparation of porous ceramics, and thus to combine the generally superior mechanical properties of the gelcast material with the functionalities of cellular materials (light weight, low thermal conductivity, low elastic modulus and, possibly, fluid permeability) [36,37].
While the toughening effect of grains of the second phase in dense alumina matrices has been well investigated, few papers are available on porous alumina-based composites [38-43].

Materials and methods

A commercial α-alumina powder (A, TM-DAR TAIMICRON, supplied by Taimei Chemicals Co., Japan) was used to develop a 90 vol% alumina and 10 vol% of ZrO_2 (AZ) composite by surface modification [28,44]. First, the alumina powder was dispersed in distilled water under magnetic stirring with a solid load of 65 wt% for 5 days. Particle size distribution was determined using a laser granulometer (Fristch Analysette 22). Then, the precursor of the second phase, a 3M $ZrCl_4$ (Fluka, > 98% purity) aqueous solution, is drop-wise added to the alumina slurry to obtain the AZ composite powder. The amount of $ZrCl_4$ was calculated assuming that zirconia was fully tetragonal in the final composites, so that a α-Al_2O_3 to $ZrCl_4$ weight ratio of 1:0.636 was employed.

The addition of zirconium chloride decreased the pH of the suspension to values lower than 1. Thus, to avoid possible corrosion of the spray-dryer (Mini Spray Dryer Buchi B-290) steel parts, it was necessary to add a basic complexing agent to increase the pH to about 4.5. For this reason, tribasic ammonium citrate (Sigma, ≥ 97% purity) was also added to the doped alumina suspension. After homogenization under magnetic stirring for 2 h, the suspension was diluted down to 4 wt% and spray dried.

The dried doped powder was then calcined at 600°C to induce chloride decomposition as well as solid-state reaction to yield the final phases. More details about the composite powders elaboration can be found in [28-30,44]. The powders were analyzed by X-ray diffraction (Philips PW 1710) with a Cu Kα anticathode (λ=0.154056 nm) in the 5-70° range in 2 theta, a scan speed of 0.04°/step and a time per step of 2.5 s.

The doped powder was then dispersed by ball milling with a solid load of 65 wt%. An agar (A7049 from Sigma-Aldrich) was used as the gelling agent, and polyethylene spheres (Clariant Italia SpA) were used as the fugitive phase. To control the pore diameter in the final components, polyethylene spheres were sieved in the range 224-355 μm and then added to the dispersed ceramic slurry in suitable amounts to obtain fired ceramics with about 65-70-75 vol% porosity. SEM observations (SEM, Hitachi S2300) were used to measure the size distribution of the PE spheres by means of image analysis software (Scandium by Soft Image System) on about 300 spheres.

The agar was dissolved into distilled water at 90°C, cooled down to 60°C and then added to the ceramic suspension, at the same temperature. In this way an amount of gelling agent of 0.5 wt%, with respect to the final water content, and a final ceramic solid content of 50 wt% and 44 wt% for alumina and the biphasic composite powder, respectively, were reached. It is important, in this process, to have as high as possible solids loading in the slurry to minimize shrinkage and warpage

during drying and to enhance fired density. At the same time, it is necessary that the suspension remains fluid and pourable [4]. For this reason, the viscosity of the ceramic slurries at 60°C was measured using a viscometer (Brookfield HBDV-II), before and after the agar addition. After a pre-shear, the apparent viscosity was measured at shear rates ranging from 6.12 to 245 s^{-1}, maintaining each value constant for 10 s.

Casting of the suspensions was carried out under vacuum (about 10^{-2} Pa) to remove air bubbles entrapped in the ceramic suspension. Cylindrical Plexiglas molds having internal diameter of 1.5 cm and height of 5 cm were used. The drying step is a crucial step of the gelcasting process and it has to be done at high relative humidity (RH > 90%) until shrinkage has stopped to minimize warpage and cracking [4] due to non-uniform and differential drying in various regions because of the solvent gradient [45]. Then, the drying rate is increased either by raising the temperature or decreasing the RH, or a combination of both. In our case, the cast samples were first dried at high RH for two days, and after demolding the RH was slowly decreased.

Some dense gelcast materials were prepared without the PE spheres in the ceramic suspension and submitted to dilatometric studies (Netzsch 402E), heating up to 1500°C with a holding time of 3 hrs, with a heating rate of 10°C/min up to 1100°C and 2°C/min up to the maximum temperature. A 10°C/min cooling rate was finally used.

On the basis of the dilatometric studies, porous materials were sintered at 1400°C for 1 h in the case of A samples, and at 1550°C for 3 hrs in the case of AZ samples (in all the cases with a heating rate of 2°C/min and a cooling rate of 5°C/min [46]). To control the thermal decomposition of polyethylene spheres without damaging the green ceramic structure, various intermediate steps below 600°C were carried out [25, 47].

The density of the green and fired components was evaluated using weight and geometrical measurements as well as Archimedes method (for sintered samples only). The total porosity and the closed porosity were calculated as follow:

$$Total\ porosity\ (\%) = \left(1 - \frac{\text{Geometrical density}}{\text{Theoretical density}}\right) \times 100 \quad (1)$$

$$Closed\ porosity\ (\%) = \left(1 - \frac{\text{Archimedes density}}{\text{Theoretical density}}\right) \times 100 \quad (2)$$

The materials microstructures were observed by scanning electron microscopy. The image analysis (Scandium by Soft Image System), performed on several SEM micrographs of polished surfaces of the fired components (measuring about 400 pores for each composition), allowed evaluation of the pore size distribution. These results, obtained from 2D sections, led to a pore size distribution related, but not equivalent, to the real diameters in the 3D space.

The mechanical properties were investigated by uniaxial compressive tests (Instron 4201; the measurements were made in displacement control mode and the load was applied at a crosshead rate of 1 mm/min).

Results

X-Ray diffraction patterns of the powders reveal the presence of α-alumina phase and of the tetragonal ZrO_2 for AZ.

The dispersion of the ceramic powder suspensions was verified by laser granulometry: the particle size distributions of the A and AZ dispersions reach almost the same values of the diameters corresponding to 10, 50, 90% and is equal to 0.30, 0.45 and 0.87 μm, respectively for A and to 0.30, 0.49 and 1.03 μm, respectively for AZ.

In addition, to establish the solid load suitable for the gelcasting procedure, the viscosities of ceramic suspensions having different weight fractions of powder were measured, before and after the agar addition. Figure 1 shows the effect of the gelling agent, using the alumina slurry as an example. Even if a very low viscosity is measured for the ceramic suspension, a significant increase is recorded after the agar addition. The A and AZ slurries with a solid load of 50 wt% and 44 wt%, respectively, are characterized by an apparent viscosity lower than 1000 mPa.s at 20 s^{-1}, which is suitable for the casting process [48].

On the basis of these results, after dispersion, the ceramic solid content of the A and AZ suspensions is then corrected to the final values of 50 wt% and 44 wt%, respectively.

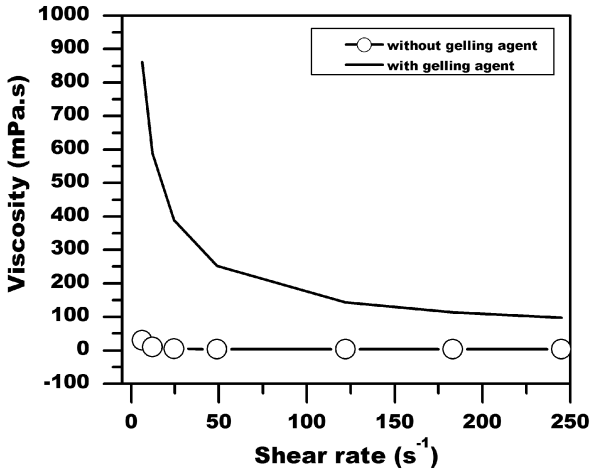

FIGURE 1: Viscosity of dispersed suspensions of alumina, with a solid content of 50 wt%, before and after agar addition

The SEM observations of the PE spheres revealed that sieving was not effective in assuring a controlled selection of particle diameters: the particle size distribution (Figure 2) showed that a non negligible fraction of spheres had diameters below 224 μm.

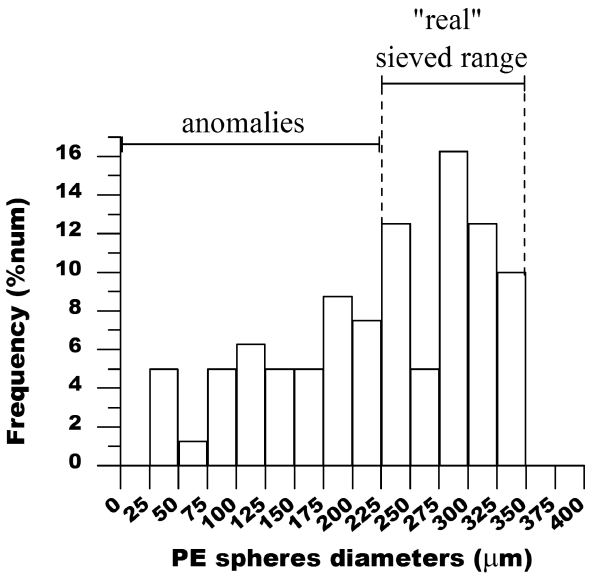

FIGURE 2: Particle size distribution of the selected fraction of PE spheres

To investigate the densification behavior, some dense A and AZ materials were prepared by the gelcasting procedure described above, without adding the PE spheres in the ceramic suspension, and were submitted to dilatometric analyses.

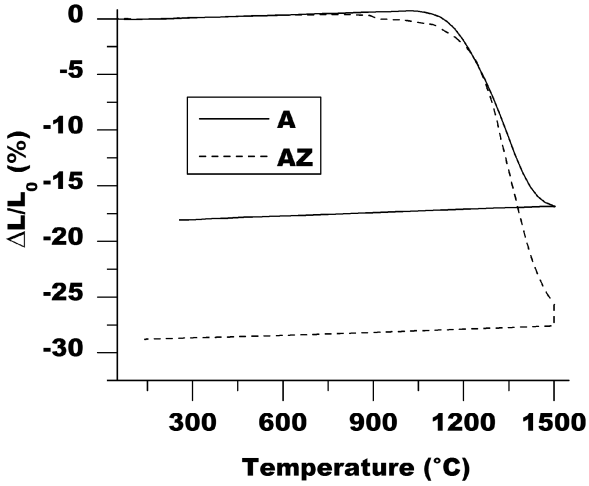

FIGURE 3: Dilatometric curves of dense gelcast A and AZ materials

As shown in Figure 3, at 1500°C for 3 hrs, the AZ sample undergoes a higher shrinkage (about 29%) than the A material (about 18%). Notwithstanding this, the AZ specimen reaches a lower density (of about 94 TD%, referred to the theoretical value of 4.19 g/cm^3), starting from a green density of about 40 TD% than the A bar (of about 99 TD%, referred to the theoretical value of 3.98

g/cm^3), starting from a green density of about 50 TD%. On the basis of these results, the sintering conditions are fixed at 1400°C for 1 h in the case of the gelcast A materials to limit the possible grain growth, and at 1550°C for 3 hrs for gelcast AZ samples to further increase the fired density. In these conditions, both gelcast dense materials reached a density of around 93 TD%.
SEM observations on a dense AZ gelcast sample showed that the process is able to lead to a fine grained microstructure with a homogeneous distribution of the second phase (Figure 4).

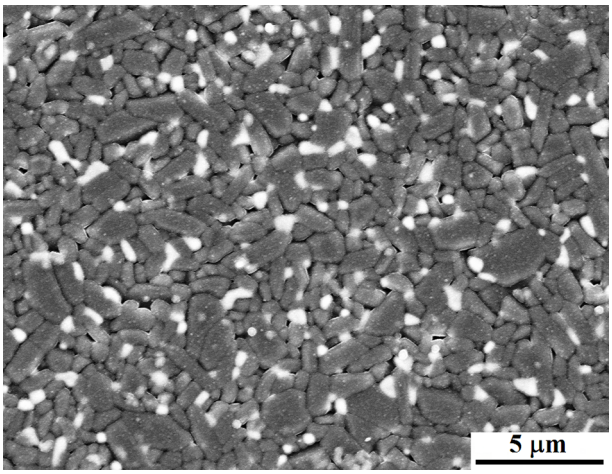

FIGURE 4: SEM micrograph of the microstructure of the dense gelcast AZ sample after sintering at 1550°C for 3 hrs (alumina grains appear in dark, zirconia ones in white)

For each ceramic powder, porous components with different amounts of PE are then prepared.
The mean values of the relative densities, before and after sintering, and porosity for the two compositions are reported in Table 1. In the case of the green components, the theoretical densities are estimated by applying the rule of mixtures for composite systems, on the basis of the ceramic and PE volume fractions and using density values of 0.93, 3.98 and 4.19 g/cm^3 for PE, A and AZ, respectively.

TABLE 1: Mean values of the relative densities and porosity

	Green geometrical density [g/cm^3 (%TD)]	Fired geometrical density [g/cm^3 (%TD)]	Total porosity [%]	Fired Archimedes density [g/cm^3 (%TD)]	Closed porosity [%]
A65	1.14±0.11 (58.7±4.5)	1.51±0.20 (38.0±5.0)	62	2.25±0.27 (56.6±6.8)	43
A70	1.01±0.04 (53.2±2.6)	1.17±0.05 (29.5±1.4)	70	2.49±0.20 (62.6±5.0)	37
A75	0.80±0.04 (47.2±2.4)	0.67±0.05 (16.9±1.3)	83	3.48±0.16 (87.5±4.0)	12
AZ65	1.09±0.04 (54.4±3.2)	1.86±0.10 (44.3±2.3)	56	2.57±0.05 (61.9±1.9)	38
AZ70	1.04±0.05 (53.7±3.0)	1.69±0.14 (40.4±3.3)	60	2.57±0.06 (64.1±2.2)	36
AZ75	0.84±0.06 (48.0±3.4)	1.15±0.11 (27.3±2.6)	73	3.15±0.13 (75.1±3.2)	25

As illustrated in Table 1, even if the PE amount is strictly controlled, lower porosity volumes are created during the sintering treatment of the AZ materials.

The SEM observations of the porous materials revealed a good distribution of the macro-pores (Figure 5a-f) and the presence of a diffuse micro-porosity with dimensions of about 1 μm (Figure 5g and h), probably due to the use of the agar as the gelling agent [50].

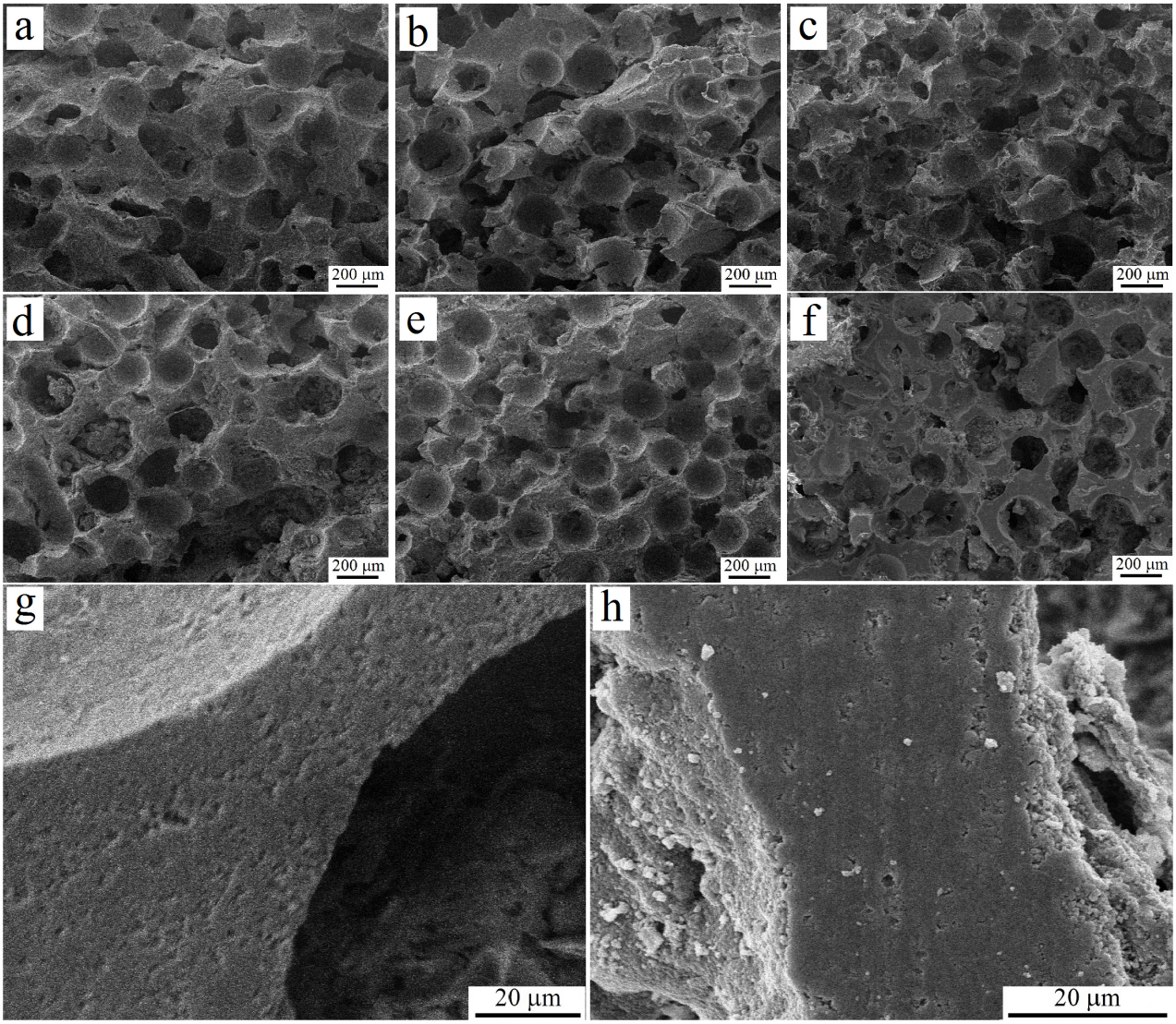

FIGURE 5: SEM images of: a) A65, b) A70, c) A75, d) AZ65, e) AZ70, f) AZ75 samples; higher magnification images of: g) A and h) AZ struts

The SEM image analysis reveals that the porous materials present a different pore size distribution, as illustrated in Figure 6; in fact A samples show larger pore diameters, with a mean value of about 190 µm, whereas lower values are determined for the AZ specimens, in which a mean diameter of 130 µm is observed.

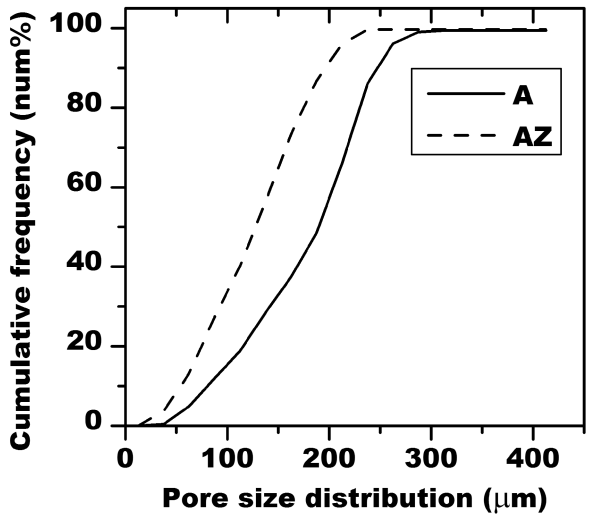

FIGURE 6: Apparent pore size distribution of A and AZ materials by SEM images

The compressive stress-strain curves for the A and AZ materials, at porosities of 60 and 70 vol% are shown in Fig. 7. The maximum stress reaches mean values of 24.4 and 35.1 MPa for A and AZ, respectively, when the porosity is about 60 vol%. On the other hand, maximum stress mean values of 3.7 and 4.5 MPa were reached for A and AZ, respectively, when the porosity is about 70 vol%.

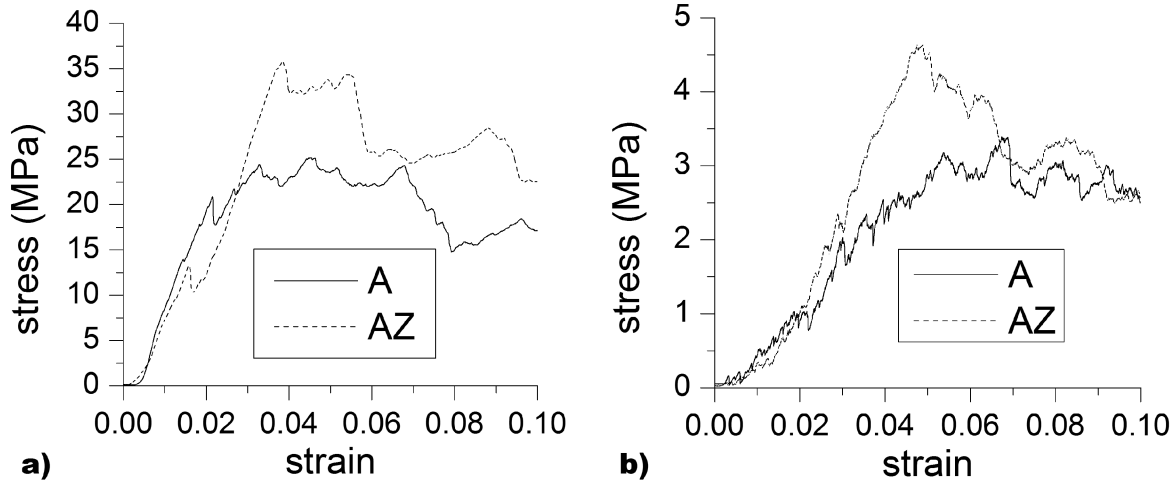

FIGURE 7: compressive curve of A and AZ samples with a porosity of: a) 60 vol% and b) 70 vol%

Figure 8 shows the mechanical behavior of the A and AZ samples as a function of the relative density.

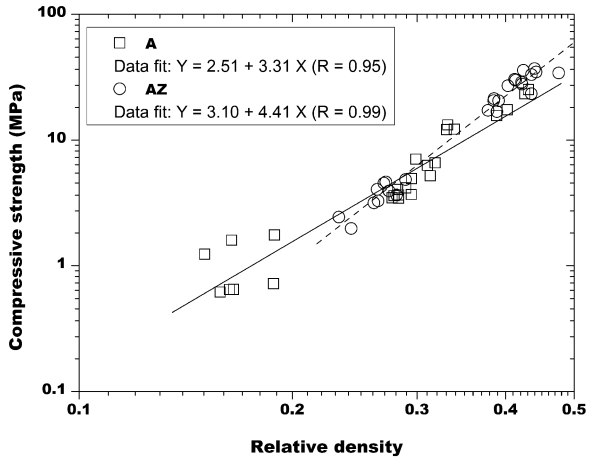

FIGURE 8: Compressive strength as a function of the relative density of A and AZ materials, plotted on log scales.

For the two investigated compositions, the compressive strength increases with the relative density decreases. The power dependence of strength on relative density from log-log plot of Figure 6 are equal to 3.3 and 4.4, respectively for A and AZ samples.

Discussion

The pore dimensions in the porous ceramics depend on the starting particle size distribution of the PE spheres (which was the same for all the porous materials) and on the shrinkage that the ceramic walls undergo during sintering. As shown in Figure 3, the AZ material undergoes the highest shrinkage; consequently, the pore size distribution of this type of porous material is shifted to lower values (Figure 6). On the other hand, larger pores are observed (Figure 6) in the case of A materials, compatible with the limited shrinkage (Figure 3).

As shown in Figure 7, the stress-strain curves of the porous ceramics made in this study are typical of foams: a linear elastic region is recorded at low stresses, then the ceramic struts progressively break and damage accumulates layer by layer [36]. The materials undergo a progressive collapse, with the formation and propagation of cracks in the cell walls [49]. The porosity and the composition of the ceramic influence the mechanical behavior of these materials.

On the ground of SEM observations, shown in Figure 5, it is possible to observe an increase in the interconnections among the pores, and consequently a decrease of the volume fraction of the solid phase, as the amount of the fugitive phase increases.

An estimation of the average wall thickness and its dependence on the relative porosity can be obtained using the following equation [49]:

$$e = \Phi\left(\left(\frac{P_{\max}}{P}\right)^{1/3} - 1\right) \quad (3)$$

where: e is the wall thickness,

Φ the mean pore diameter evaluated by image analysis,

P_{max} the maximum porosity, calculated with the maximal packing of pores without interpenetration and equal to 0.8 [49],

p the total porosity reported in Table 1.

When the pore volume increases, the mean distance between two neighboring pores and, consequently, the wall dimensions decrease [49]. This is shown for the A and AZ materials in Figure 9, which also highlights the influence of the pore diameter. In fact, the AZ components present smaller pores and, consequently, smaller struts among them with respect to the A samples.

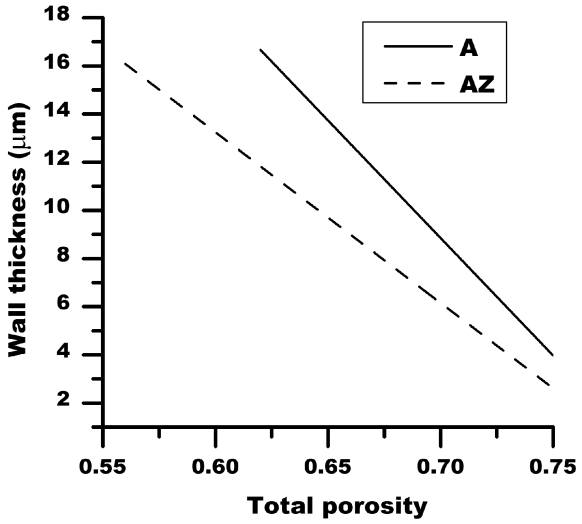

FIGURE 9: The wall sizes as a function of the total porosity of A and AZ materials, according to equation (3).

Moreover, considering that in this type of porous material the mechanical properties also depend on the distribution of the solid in the cell walls [49]. The diffuse micro-porosity present in the strut microstructure (Fig. 5g and h) of the A and AZ materials, decreases the mechanical properties of the solid cell wall.

From a compositional point of view, considering the effect of the dispersion of fine ZrO_2 grains in an alumina matrix on its mechanical behavior [33-35], the formation and propagation of the cracks in the ceramic walls of the porous components could be controlled by the exploitation of alumina-zirconia composites.

The different compressive behavior of A and AZ components are mainly evident at lower porosity levels, as illustrated in Figure 7. In fact, for 60 vol% samples, the area under the stress strain curves is higher for AZ with respect to A compositions, and as it is proportional to the work of fracture, one can expect that the composite porous ceramics present not only higher compressive strengths, but are also less brittle. This result is probably due the effective reinforcement of the second phase. This behavior is also observed in the stress-strain curves of the 70 vol% porous materials (Figure 7b), even if the decrease in wall thickness makes it less evident.

The calculated values of n, the exponent indicating the power dependence of strength on relative density from log-log plot of Figure 6, equal to 3.3 and 4.4, respectively for A and AZ samples, are different from the exponent of the Gibson and Ashby model (1.5) for open cellular ceramics with a constant cell size. Such a difference can be attributed to the different nature of the porosity, which in these materials is not exclusively open, as in the case of Gibson and Ashby model, and to the cell features (size distribution, non-periodic and disordered distribution, volume fraction of solids in the cell faces), as well as to the presence of closed voids or defects in the struts, as reported in the literature [51, 52, 53]. These n values are close to the one obtained by Colombo et al. on silicon oxycarbide ceramic foams (3.6) [53].

Conclusions

The modified gelcasting process based on an agar as natural gelling agent and polyethylene spheres as pore formers, is useful for the production of homogeneous porous composite materials. SEM observations on a dense AZ gelcast sample showed that the process leads to a fine grained microstructure with a homogeneous distribution of the second phase. The porosity features such as the amount of porosity, the pore shape and size distribution can be easily controlled by adding a fixed amount of polyethylene spheres sieved in a restricted dimensional range. For all the examined compositions, the strength decreases by decreasing the relative density. From a compositional point of view, considering the effect of the dispersion of fine ZrO_2 grains in an alumina matrix on its mechanical behavior, the formation and propagation of the cracks in the ceramic walls of the porous components could be controlled by the exploitation of alumina-zirconia composites.

Acknowledgements

Prof. Lorna J. Gibson, prof. Jean-Marc Tulliani and Dr. Mariangela Lombardi gratefully acknowledge the MITOR Project, which supports research collaborations and exchanges between

the Massachusetts Institute of Technology (MIT) and the Politecnico di Torino, thanks to the generous support of the Compagnia di San Paolo.

References

[1] M.A. Janney, Method for molding ceramic powders, US Patent 4,894,194 (1990)

[2] M.A. Janney, O.O. Omatete, Method for molding ceramic powders using a water-based gel casting, US Patent 5,028,362 (1991)

[3] A.C. Young, O.O. Omatete, M.A. Janney, P.A. Menchhofer, Gelcasting of alumina, Journal of the American Ceramic Society, 74 [3] (1991) 612-618

[4] O.O. Omatete, M.A. Janney, S.D. Nunn, Gelcasting: From laboratory development toward industrial production, Journal of the American Ceramic Society, 17 (1997) 407-413

[5] M. Potoczek, E. Zawadzak, Initiator effect on the gelcasting properties of alumina in a system involving low-toxic monomers, Ceramics International, 30 (2004) 793-799.

[6] K. Cai, Y. Huang, J. Yang, Alumina gel casting by using HEMA system, Journal of the European Ceramic Society, 25 (2005) 1089-1093

[7] Gelcasting performance of alumina aqueous suspensions with glycerol monoacrylate: A new low-toxicity acrylic monomer, Journal of the American Ceramic Society, 90 [5] (2007) 1386-1393

[8] K. Prabhakaran, C. Pavithran, Gel casting of alumina from acidic aqueous medium using acrylic acid, Journal of the European Ceramic Society, 20 (2000) 1115-1119

[9] C. Zhang, J. Yang, T. Qiu, J. Guo, Preparation of ZTA ceramic by aqueous gelcasting with a low-toxicity monomer DMAA, Ceramics International, 38, 4 (2012)3063-3068.

[10] X. J. Mao, S. Z. Shimai, M. J. Dong, and S. W. Wang, Gelcasting of alumina using epoxy resin as gelling agent, Journal of the American Ceramic Society, 90 [3] (2007) 986–8

[11] K. Prabhakaran, C. Pavithran, Gel casting of alumina using urea-formaldehyde II. Gelation and ceramic forming, Ceramics International, 26 (2000) 67-71

[12] L. Wu, Y. Huang, Z. Wang, L. Liu, Controlled fabrication of porous Al2O3 ceramic by N,N'-dimethylformamide-based gel-casting, Scripta Materialia, 62 (2010) 602-605

[13] A.J. Millán, R. Moreno, M.I. Nieto, Thermogelling polysaccharides for aqueous gelcasting-part I: a comparative study of gelling additives, Journal of the European Ceramic Society, 22 (2002) 2209-2215

[14] S. Dhara, P. Bhargava, Egg white as an environmentally friendly low-cost binder for gelcasting of ceramics, Journal of the American Ceramic Society, 84 [12] (2001) 3048-3050

[15] M. Bengisu, E. Yilmaz, Gelcasting of alumina and zirconia using chitosan gels, Ceramics International, 28 (2002) 431-438

[16] Y. Chen, Z. Xie, J. Yang, Y. Huang, Alumina casting based on gelation of gelatine, Journal of the European Ceramic Society, 19 (1999) 271-275
[17] Z. Xie, Y. Chen, Y. Huang, A novel casting forming for ceramics by gelatine and enzyme catalysis, Journal of the European Ceramic Society, 20 (2000) 253-257
[18] Y. Jia, Y. Kanno, Z. Xie, New gel-casting process for alumina ceramics based on gelation of alginate, Journal of the European Ceramic Society, 22 (2002) 1911-1916
[19] F.S. Ortega, F.A.O. Valenzuela, C.H. Scuracchio, V.C. Pandolfelli, Alternative gelling agents for the gelcasting of ceramic foams, Journal of the European Ceramic Society 23 (2003) 75-80
[20] J. Wang, X. Wang, W. Zhao, Alumina gelcastin g by using glutin-urea system, Advanced Materials Research, v 284-286 (2011) 1423-1426.
[21] P. Bednarek, M. Szafran, Y. Sakka, T. Mizerski, Gelcasting of alumina with a new monomer synthesized from glucose, Journal of the European Ceramic Society, 30, 8 (2010) 1795-1801.
[22] H. R. Ramay, M. Zhang, Preparation of porous hydroxyapatite scaffolds by combination of the gel-casting and polymer sponge methods, Biomaterials, 24 (2003) 3293–3302.
[23] C. Chuanuwatanakul, C. Tallon, D.E. Dunstan, G.V. Franks, Controlling the microstructure of ceramic particle stabilized foams: Influence of contact angle and particle aggregation, Soft Matter, 7, 24 (2011) 11464-11474.
[24] F. Li, H. Ni, J. Wang, B. Sun, Z. Du, Gelcasting of aqueous mesocarbon microbead suspension, Carbon, 42, 14 (2004) 2989–2995
[25] M. Lombardi, V. Naglieri, J.M. Tulliani, L. Montanaro, Gelcasting of dense and porous ceramics by using a natural gelatine, Journal of porous materials, 16 (2009) 393-400
[26] X. Guo, Z. Zhou, S. Wang, S. Zhao, Q. Zhang, G. Ma, A novel method for preparation of interconnected pore-gradient ceramic foams by gelcasting, Journal of Porous Materials, available online.
[27] Yang, J., Yu, J., Huang, Y. Recent developments in gelcasting of ceramics *JECS*, Vol. 31, No. 14, 2011, pp. 2569-2591
[28] Palmero P, Kern F, Lombardi M, Gadow R. Role of immiscible and miscible second phases on the sintering kinetics and microstructural development of nano-crystalline α-Al_2O_3-based materials. Ceram Int 2011;37:3547-56.
[29] Palmero P, Esnouf C. Phase and microstructural evolution of yttrium-doped nanocrystalline alumina: A contribution of advanced microscopy techniques. J Eur Ceram Soc 2011;31:507-16.
[30] Palmero P, Naglieri V, Spina G, Lombardi M. Microstructural design and elaboration of multiphase ultra-fine ceramics. Ceram Int 2011;37:139-44.

[31] Palmero P, Montanaro L. Thermal and mechanical-induced phase transformations during YAG and alumina-YAG syntheses. J Therm Anal Calorim 2007;88:261-7.
[32] Palmero P, Sola A, Naglieri V, Bellucci D, Lombardi M, Cannillo V. Elaboration and mechanical characterization of multi-phase alumina-based ultra-fine composites. J Mater Sci 2012;47:1077-84.
[33] Chevalier J, Grandjean S, Kuntz M, Pezzotti G. On the kinetics and impact of tetragonal to monoclinic transformation in an alumina/zirconia composite for arthroplasty applications. Biomaterials 2009;30:5279–82.
[34] Sadangi RK, Shukla V, Kear BH. Processing and properties of $ZrO_2(3Y_2O_3)$–Al_2O_3 nanocomposites. Int. J Refract Met Hard Mater 2005;23:363–8.
[35] Kern F, Palmero P. Microstructure and mechanical properties of alumina 5 vol% zirconia nanocomposites prepared by powder coating and powder mixing routes. Ceram Int 2012 in press.
[36] Gibson LJ, Ashby MF. Cellular solids – structure and properties. Second editions, Cambridge: Cambridge University Press 1997; p. 93-344.
[37] Scheffler M, Colombo P, editors. Cellular ceramics. Weinheim: Wiley-VCH; 2005. p. 3-17, 225-400.
[38] Vogt UF, Gorbar M, Dimopoulos-Eggenschwiler P, Broenstrup A, Wagner G, Colombo P. Improving the properties of ceramic foams by a vacuum infiltration process. J Eur Ceram Soc 2010;30:3005-11.
[39] Pabst, W., Gregorová, E., Sedlàřovà, I., Preparation and characterization of porous alumina–zirconia composite ceramics, *JECS*, Vol. 31, No. 14, 2011, pp. 2721-2731
[40] U.F. Vogt, M. Gorbar, P. Dimopoulos-Eggenschwiler, A. Broenstrup, G. Wagner, P. Colombo, Improving the properties of ceramic foams by a vacuum infiltration process, Journal of the European Ceramic Society 30 (2010) 3005–3011
[41] Liu G, Zhang D., Meggs C, Button TW. Porous Al_2O_3-ZrO_2 composites fabricated by an ice template method. Scripta Mater 2010;62:466-8.
[42] Sopyan I, Fadli A, Mel M. Porous alumina-hydroxyapatite composites through protein foaming-consolidation method. J Mech Behav Biomed 2012;8:86-98.
[43] Yang Y, Wang Y, Tian W, Wang Z, Li C, Zhao Y, Bian H. In situ porous alumina-aluminum titanate ceramic composite prepared by spark plasma sintering from nanostructured powders. Scripta Mater 2009;60:578-81.
[44] Naglieri V, Palmero P., Montanaro L. Preparation and characterization of alumina-doped powders for the design of multi-phasic nano-microcomposites. J Therm Anal Calorim 2009;97:231-7.

[45] A. Barati, M. Kokabi, M. Hossein Navid Famili, Forming alumina parts using acrylamide gels, Iranian Polymer Journal, 12 (2) (2003) 127-138
[46] Palmero P, Lombardi M, Montanaro L, Azar M, Chevalier J, Garnier V, Fantozzi G. Effect of heating rate on phase and microstructural evolution during pressureless sintering of a nanostructured transition alumina. Int J Appl Ceram Tec 2009;6:420-30.
[47] J.M. Tulliani, C. Bartuli, E. Bemporad, Preparation and mechanical characterization of dense and porous zirconia produced by gel casting with gelatin as a gelling agent, Ceramics International,35 (2009) 2481-2491.
[48] C. Ha, Y. Jung, J. Kim, C. Jo, and U. Paik. Effect of particle size on gelcasting process and green properties in alumina. Materials Science Engineering A 337, 212 (2002)
[49] S. Meille, M. Lombardi, J. Chevalier, L. Montanaro. Mechanical properties of porous ceramics in compression: On the transition between elastic, brittle, and cellular behavior. Journal of the European Ceramic Society, 2012, in press.
[50] C. Bartuli, E. Bemporad, J.M. Tulliani, J. Tirillò, G. Pulci, M. Sebastiani, Mechanical properties of cellular ceramics obtained by gel casting: Characterization and modeling, Journal of the European Ceramic Society 29 (2009) 2979–2989
[51] P. Sepulveda, J.G.P. Binner, Processing of cellular ceramics by foaming and in situ polymerisation of organic monomers, J. Eur. Ceram. Soc. Vol. 19 (1999), 2059-2066
[52] F.A. Costa Oliveira, S. Dias, M. Fatima Vaz, J. Cruz Fernandes, Behaviour of open-cell cordierite foams under compression, Journal J. Eur. Ceram. Soc., Vol. 26 (2006), 179-186
[53] P. Colombo, J. R. Hellmann, D. L. Shelleman, Mechanical Properties of Silicon Oxycarbide Ceramic Foams, J. Am. Ceram. Soc., 84 [10] 2245–51 (2001)

Figures caption

FIGURE 1: Viscosity of dispersed suspensions of alumina, with a solid content of 50 wt%, before and after agar addition

FIGURE 2: Particle size distribution of the selected fraction of PE spheres

FIGURE 3: Dilatometric curves of dense gelcast A and AZ materials

FIGURE 4: SEM micrograph of the microstructure of the dense gelcast AZ sample after sintering at 1550°C for 3 hrs (alumina grains appear in dark, zirconia ones in white)

FIGURE 5: SEM images of: a) A65, b) A70, c) A75, d) AZ65, e) AZ70, f) AZ75 samples; higher magnification images of: g) A and h) AZ struts

FIGURE 6: Apparent pore size distribution of A and AZ materials by SEM images

FIGURE 7: compressive curve of A and AZ samples with a porosity of: a) 60 vol% and b) 70 vol%

FIGURE 8: Compressive strength as a function of the relative density of A and AZ materials, plotted on log scales.

FIGURE 9: The wall sizes as a function of the total porosity of A and AZ materials, according to equation (3).